Research Article

Journal of Environmental Nanotechnology

Green Synthesis of Multifunctional Carbon Nanodots from *Phyla nodiflora* Leaf Extract and their Potential Applications

A. Mushira Banu, S. Jayathivya*, B. Arifa Farzana and M. Kathiravan

PG and Research Department of Chemistry, Jamal Mohamed College (A), Affiliated to Bharathidasan University, Tiruchirappalli, TN, India

Received: 26.01.2025 Accepted: 18.03.2025 Published: 30.03.2025

*jayathivya3@gmail.com

ABSTRACT

This study focuses on the synthesis and characterization of carbon nanodots derived from *Phyla nodiflora* leaves, a naturally abundant and sustainable precursor. *Phyla nodiflora* leaves are rich in bioactive compounds, such as polyphenols, flavonoids, triterpenes, and saponins. Carbon Nanodots (CNDs) exhibited strong blue-green fluorescence, high quantum yield, and excellent photostability, making them suitable for multifunctional applications. In this research work, CNDs were synthesized from *Phyla nodiflora* leaf extract using a one-step hydrothermal method to produce highly fluorescent CNDs with remarkable physicochemical properties. Comprehensive characterization techniques, including UV, Fourier-transform infrared spectroscopy and fluorescence studies, revealed the surface functional groups and heteroatom doping of the CNDs. The presence of oxygen- and nitrogen-containing groups, naturally doped into the CNDs during synthesis, was attributed to the phytochemical composition of *Phyla nodiflora* leaves, enhancing their optical and catalytic properties. This study also explores the application of PN-CNDs as a corrosion inhibitor for mild steel in a 1.0 M HCl solution. PN-CNDs were found to be effective in improving corrosion resistance, as evidenced by electrochemical measurements showing a significant increase in polarization resistance and a decrease in corrosion current density. By tackling corrosion-related issues in a range of industrial applications, this research aids in the development of sustainable materials for corrosion protection. The equilibrium data were analyzed using the Langmuir isotherm model to determine the adsorption capacity and surface heterogeneity. Furthermore, structural evaluations using scanning electron microscopy validated the dependability on PN-CNDs-C's as a corrosion barrier.

Keywords: *Phyla nodiflora;* Carbon nanodots; Biomass precursor; Corrosion.

1. INTRODUCTION

Carbon nanodots (CNDs) are a class of zero-dimensional carbon-based nanomaterials with unique optical, electronic, and chemical properties. These properties make them valuable in a range of applications, including bioimaging, sensing, environmental monitoring, and drug delivery. Carbon nanodots have gained significant attention in recent years as promising materials for a wide array of applications in bioimaging, biosensing, drug delivery, and energy systems. These zero-dimensional nanomaterials are known for their remarkable photoluminescent properties, high biocompatibility, ease of functionalization, and cost-effective synthesis processes. Their environmentally friendly nature and potential for scaling up production further add to their appeal, particularly in developing green and sustainable technologies. Plant-based synthesis routes offer several advantages, including sustainability, simplicity, and the presence of natural stabilizing and reducing agents in plant extracts. Among the myriads of plant sources explored, Poduthalai (*Phyla nodiflora*), a traditional medicinal plant, has recently gained attention for its rich phytochemical content. This plant is known for its bioactive compounds, which can act as both reducing and capping agents during the synthesis of nanomaterials. The use of Poduthalai leaves as a green precursor for synthesizing carbon nanodots holds immense potential due to their high content of bioactive compounds, which aid in reducing carbon sources into nanoscale structures and provide stability to the synthesized nanodots. These naturally derived nanomaterials are anticipated to exhibit enhanced biocompatibility and reduced cytotoxicity, making them suitable for biomedical applications. Furthermore, the incorporation of such natural sources aligns with sustainable development goals by reducing reliance on chemical synthesis processes that often involve hazardous reagents (Bhunia *et al*. 2013; De and Karak, 2017; Chan *et al*. 2018; Amjad *et al*. 2019).

This research aims to develop and characterize advanced carbon nanodots derived from Poduthalai leaves using a simple, cost-effective, and environmentally friendly synthesis approach. The study focuses on evaluating the optical, structural, and functional properties of these CNDs and exploring their potential applications in areas such as bio-imaging and

sensing. Carbon-based nanomaterials, particularly carbon dots (CDs), have emerged as a focus of nanotechnology research due to their small size, excellent photoluminescence, high biocompatibility, and eco-friendly nature. Carbon dots are typically synthesized using physical or chemical methods; however, these approaches often involve toxic reagents and high energy consumption, which limit their sustainability. Green synthesis methods, which use natural, renewable precursors, offer a promising alternative for sustainable and environmentally friendly nanomaterial production. Green synthesis produces safer synthesis methods and products by using fewer harmful chemicals. It lowers pollution and waste generation by utilizing natural resources and effective procedures. By using renewable resources and reducing environmental effects, green synthesis encourages sustainable practices. When compared to conventional techniques, the use of natural reagents and effective procedures helps to reduce the carbon footprint. This method is less expensive than conventional techniques because it makes use of easily accessible and reasonably priced natural materials.

Plants, with their rich reservoirs of bioactive compounds such as flavonoids, tannins, and phenols, have gained attention as precursors for green nanotechnology. Among these, *Phyla nodiflora*, a traditional medicinal plant, is a promising candidate for carbon dot synthesis. Plant leaves are rich in phytochemicals that act naturally, reducing and capping agents, facilitating the production of stable, functionalized carbon dots. Utilizing this renewable resource supports the global drive toward sustainable development and green chemistry practices (Genc *et al*. 2017; Gao *et al*. 2018).

Nowadays, many efforts have been made on the development of new strategies for the synthesis and doping of CNDs. Different physical and chemical methods, such as hydrothermal treatment, laser ablation, electrochemical oxidation, and microwave treatment, have been presented in the literature. The hydrothermal method, a well-established and environmentally friendly synthesis approach, is particularly effective for producing carbon nanodots. It involves the use of high-pressure, high-temperature aqueous systems, allowing for precise control over reaction conditions and enabling the direct carbonization of natural organic matter into nanostructures. Poduthalai (*Phyla nodiflora*), a traditional medicinal plant rich in bioactive compounds such as polyphenols, flavonoids, and tannins, represents a promising natural precursor for CND synthesis. These phytochemicals act as reducing and stabilizing agents during the hydrothermal process, facilitating the formation of stable and functionalized CNDs.

In this study, the effect of extracts of the leaves of *Phyla nodiflora* as inhibitors is evaluated with a view to determining their effectiveness as biomass precursors using hydrothermal synthesis technique. These leaves offer dual advantage by utilizing the plant's abundant natural phytochemicals while supporting sustainable development goals through the reduction of chemical waste and dependence on synthetic precursors.

This green approach not only enhances the eco-friendliness of CND production but also improves the biocompatibility and functionality of the resulting CNDs, making them suitable for biomedical and environmental applications. These methods utilize renewable biomass and typically involve characterizations like UV-vis spectroscopy, FT-IR, and fluorescence to analyze structural and optical properties. These nanodots exhibit excellent luminescence, stability, and biocompatibility, making them promising for applications in industries (Guo *et al*. 2019).



Fig. 1: *Phyla nodiflora* leaves from Pudukkottai district, Tamil Nadu, India

2. EXPERIMENTAL SECTION

2.1 Collection of *Phyla nodiflora* Leaves

Fresh leaves of *Phyla nodiflora* were collected from the Pudukkottai district of Tamil Nadu. An aqueous extract of the leaves was prepared and used for the present work. The plant picture is shown in Fig. 1. Poduthalai (*Phyla nodiflora*), also known as punarnava, is valued in traditional medicine for its wide-ranging therapeutic properties. Its leaves are known for anti-inflammatory, antioxidant, antimicrobial and hepatoprotective benefits. They are often used to treat conditions such as liver disorders, skin ailments, respiratory issues, and urinary tract problems. The plant is also appreciated for its role in managing diabetes and promoting kidney health. Its bioactive compounds, including flavonoids and alkaloids, contribute to these medicinal effects. Accordingly, the objective of this study focuses on evaluating the optical, structural, and functional properties of these CNDs and exploring their

potential applications in areas such as bioimaging and sensing (Moradi *et al*. 2018).

2.2 Leaf Extract Preparation

Fresh *Phyla nodiflora* leaves were collected from a local area, ensuring they were free of any chemical contamination (e.g., pesticides or fertilizers). The leaves were thoroughly washed with distilled water to remove dirt and impurities. The cleaned leaves were air-dried in a shaded, ventilated area for 3–5 days to avoid the degradation of phytochemicals (Alternatively, drying in an oven at 40–50°C can be used to speed up the process). The dried leaves were ground into a fine powder using a blender and stored in an airtight container. These fine powders were used as a sample or the precursor for the synthesis of carbon dots. The powdered leaves were mixed with deionized water and subjected to hydrothermal treatment in an autoclave at a controlled temperature and pressure. The resulting solution was filtered, centrifuged, and dried to obtain highly luminescent carbon dots. This step was crucial in breaking down the plant material into a more manageable and homogenous form, facilitating subsequent extraction processes (Jeong *et al*. 2016; He *et al*. 2017). The centrifuge process with Poduthalai leaves is typically used for extracting bioactive compounds. The process involves preparing a leaf extract, often by grinding leaves with a solvent like water or ethanol. The mixture is then subjected to centrifugation to separate the supernatant (containing the desired phytochemicals) from solid residues. This method is widely applied in research to isolate flavonoids, alkaloids, and other therapeutic compounds for further analysis or use in medicinal formulations. In this process, 10 g of the powdered plant material were combined with 100 mL of double-distilled water, ensuring minimal interference with the extracted compounds. The mixture of *Phyla nodiflora* powder and double-distilled water was then subjected to a boiling process. The mixture was heated at 80–90°C for 30–60 minutes under constant stirring to extract the bioactive compounds and phytochemicals. The boiling process continued until the initial 100 mL of water was condensed down to 50 mL, concentrating the extracted components. Once the boiling process was complete, the resulting extract was allowed to cool naturally to room temperature. After cooling, the extract underwent a purification step. To remove any residual plant material or solid impurities, the extract was carefully filtered (Jhonsi *et al*. 2018) using Whatman filter paper. This filtration process ensured that the final extract was free from any particulate matter, leaving a clear and purified aqueous extract of *Phyla nodiflora* ready for further analysis and experimentation.

2.3 CND Synthesis Assisted by Hydrothermal

Carbon nanodots were synthesized by the hydrothermal method using *Phyla nodiflora* leaves (collected from Vayalogam, Pudukkottai district, Tamil Nadu) as a precursor and distilled water as the reactive solvent (Jiang *et al*. 2015). 2 g of fine powder of *Phyla nodiflora* leaves and 20 mL of distilled water were mixed in a 500 mL beaker, and the mixture was heated in an autoclave at a high temperature (e.g., 180°C) for several hours. And it was purified by using centrifugation and filtration to isolate the nanodots. The dried mixture was re-dissolved in 20 mL of ethanol, and the NaOH solution was then added drop by drop with constant stirring for 5 mins. It was then filtered through a Whatman 40 filter paper or a fine muslin cloth to remove insoluble residues, yielding a clear aqueous solution. After the hydrothermal synthesis, the residual material, which contained the newly formed PN-CNDs, was carefully scraped from the containers. This material was subsequently liquefied by dissolving it in ultra-pure water.

To further purify the sample and separate any dense particles, the mixture underwent a centrifugation process. To obtain PN-CNDs in their highly luminescent and finely dispersed form, the solvent containing the carbon dots was subjected to evaporation. Methanol, ethanol, and distilled water were the solvents used for the extraction process (Khan *et al*. 2019). The reaction mixture turned dark brown in color after one minute and, after two minutes, got charred and turned black, which was then cooled and extracted using ethanol. This evaporation was conducted at a controlled temperature of 80°C. After extraction, the sample was continuously stirred at 400 rpm maintaining the heating conditions. The excess ethanol was removed, and the solution was filtered, and thereby collected solutions were used for further analysis and studies. The result of this evaporation process was the formation of extremely bright carbon dots, which appeared as a black, fine dust-like material.

2.4 Electrochemical Measurements

A CHI760e electrochemical workstation with a standard three-electrode system (a saturated Ag/AgCl electrode (reference electrode), a platinum sheet (auxiliary electrode), and a mild steel substrate (1 cm^2 of exposure area, working electrode)) was used to conduct the electrochemical tests. Before the system attained a steady state, the open circuit potential (OCP) test was conducted before the electrochemical impedance spectroscopy (EIS) test. The EIS test was then conducted at OCP using a 5 mV disturbance signal and frequencies ranging from 100 kHz to 10 mHz. Zsimpwin 3.21

software was then used to analyze the EIS data (Li *et al*. 2017; Liu *et al*. 2019; Banu *et al*. 2024).

2.5 Surface Analysis

The surface morphology of specimens was examined using a scanning electron microscope (SEM, Hitachi, SU5000). To further reveal the corrosion inhibition mechanism of PN-CNDs was observed (Meng *et al*. 2019).

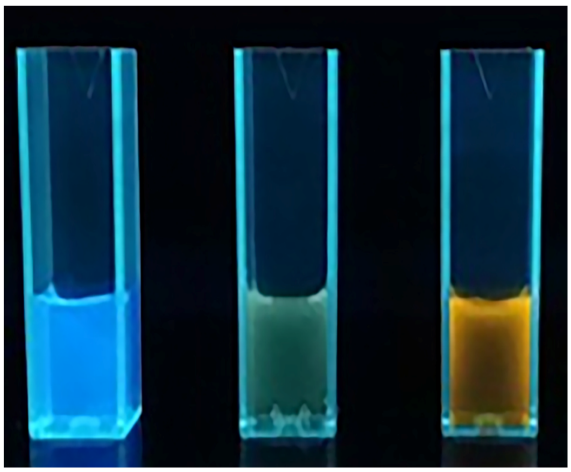


Fig. 2: Fluorescence of carbon nanodots in water, ethanol, and methanol

3. RESULTS AND ANALYSIS

3.1 UV-visible Absorption and Fluorescence Spectrum

The photoluminescence property (Fig. 2) of the newly synthesized carbon nanodots was seen in the fluorescence spectrometer. The sample was taken in the cuvette and kept under a fluorescence spectrometer with a 320–420 nm wavelength. Based on the absorption value, PL spectra (Ogi *et al*. 2016) with different excitation wavelengths such as 240, 260, 280, 300, 320, and 340 nm was noted. Carbon nanodots show a peak emission that shifts with the excitation wavelength, often appearing in the blue to green region of the spectrum. This behavior arises from surface functional groups and quantum confinement effects, highlighting their tunable fluorescence and suitability for applications like bioimaging or sensors.

UV-visible absorption (Naik *et al*. 2018) spectra were measured using Shimadzu model U–2501 PC spectrophotometer. Fluorescence spectra were measured using a Photophysics SX20 Spectrometer (Applied Photophysics Ltd, Leatherhead, United Kingdom) using a 1 cm, 4-wall transparent quartz cuvette. The purified carbon dots solution exhibited strong blue emission under UV light at 365 nm. Fig. 3a represents UV-vis spectrum of carbon nanodots synthesized from *Phyla nodiflora* leaves. It shows an absorption band around 260–280 nm due to π-π* transitions of aromatic C=C bonds, and a secondary shoulder or band near 330–350 nm related to n-π* transitions of carbonyl groups. These optical features indicate the successful formation of CNDs and their functionalized surface groups, which contribute to their fluorescence properties.

The PL excitation spectra (Fig. 3b) of CNDs were recorded at different emission wavelengths monitored from 240 to 350 nm at 20 nm intervals. The fluorescence intensity reaches its maximum when excited near the optimal wavelength (e.g., 360–400 nm). These CNDs typically exhibit strong blue or green emission with excitation-dependent fluorescence behavior.

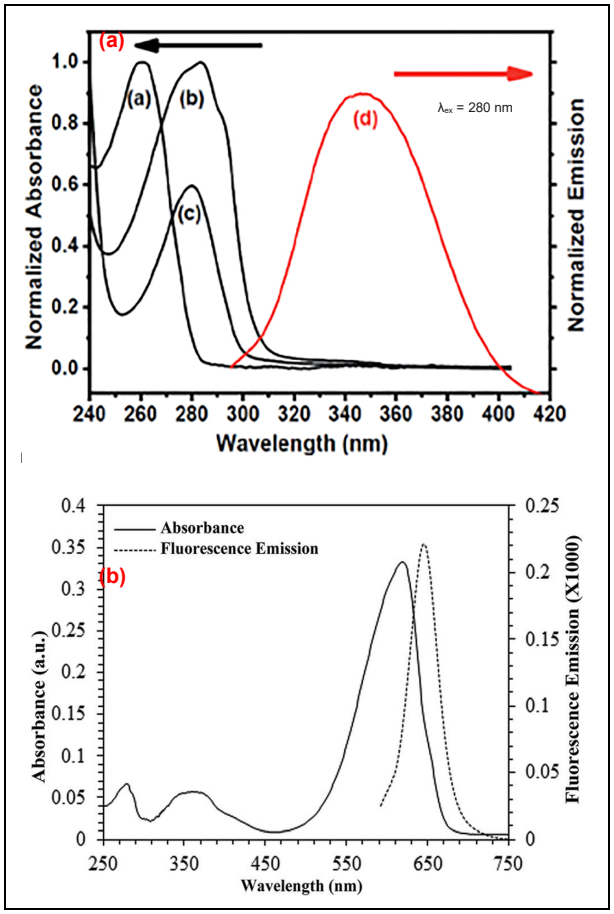


Fig. 3: Spectra of the CNDs: (a) UV-Vis absorption (b) Fluorescence emission

3.2 FT-IR Analysis

The major components present in the leaves are exhibited in Fig. 4. The IR spectrum of the synthesized carbon dots was recorded using KBr pellets as the medium with a Nicolet 380 FT-IR spectrometer (Germany). FT-IR analysis was executed to attain structural insight into the surface functionalization of C-dots. As presented in (Figs. 5a & 5b), abundant

hydrophilic groups were observed, which are designated by spectrum stretching frequencies (Quraishi *et al*. 2010) in Table 1. The presence of these functional groups ensured that the synthesized C-dots have excellent water solubility. Furthermore, the functionalized surface C-dot, in particular, the hetero groups are very useful for the interaction of the material with the metal surface. The interaction of the heteroatom with the metal surface results in the formation of an insoluble protective complex. The results revealed that these functional groups enhance water solubility, fluorescence, and surface reactivity, confirming the successful formation of functionalized CNDs suitable for various applications. The different frequencies observed in FT-IR analysis are tabulated in Table 1.

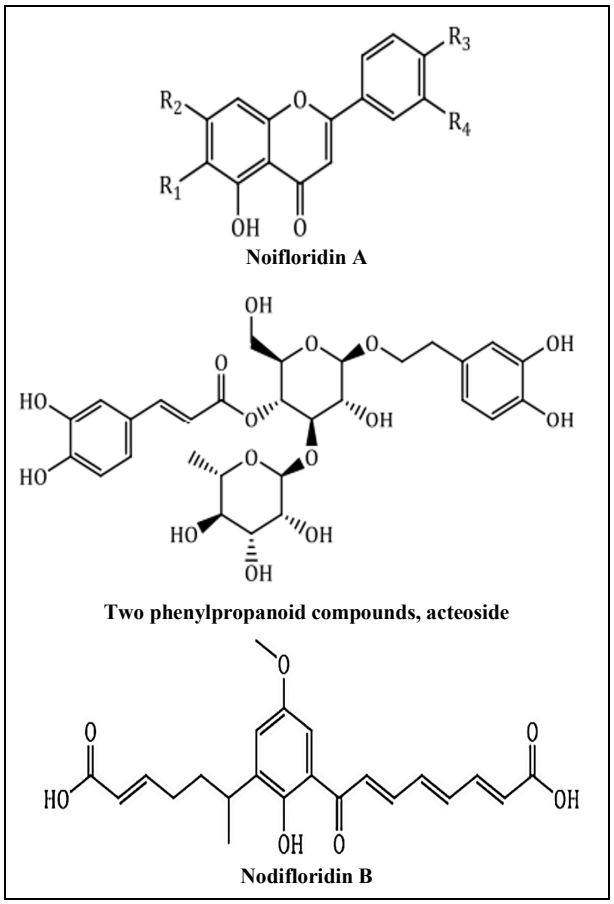


Fig. 4: Major components in *Phyla nodiflora*

Table 1. FT-IR data of PN leaves extract and PN-CNDs

Wavenumber (cm^{-1})	Functional Groups
3200–3600	O-H stretching
2800–3000	C-H stretching
1700–1750	C=O stretching
1500–1650	C=C stretching
1000–1300	C-O stretching
<1000	Fingerprint region

3.3 Electro-chemical Measurements

3.3.1 Potentiodynamic Polarization Studies

Fig. 6a shows the potentiodynamic polarization curves of mild steel in 1 M HCl solution with and without varying PN-CNDs concentrations. Table 1 lists the related electrochemical parameters and inhibition efficacy (η). The following formula was used to determine the inhibitory efficiency:

$$\eta = \frac{i^0_{corr} - i_{corr}}{i^0_{corr}} \, x \, 100 \qquad \ldots (1)$$

where i^0_{corr} and i_{corr} stand for the corrosion current density with and without PN-CNDs, respectively, and η is the inhibition efficiency.

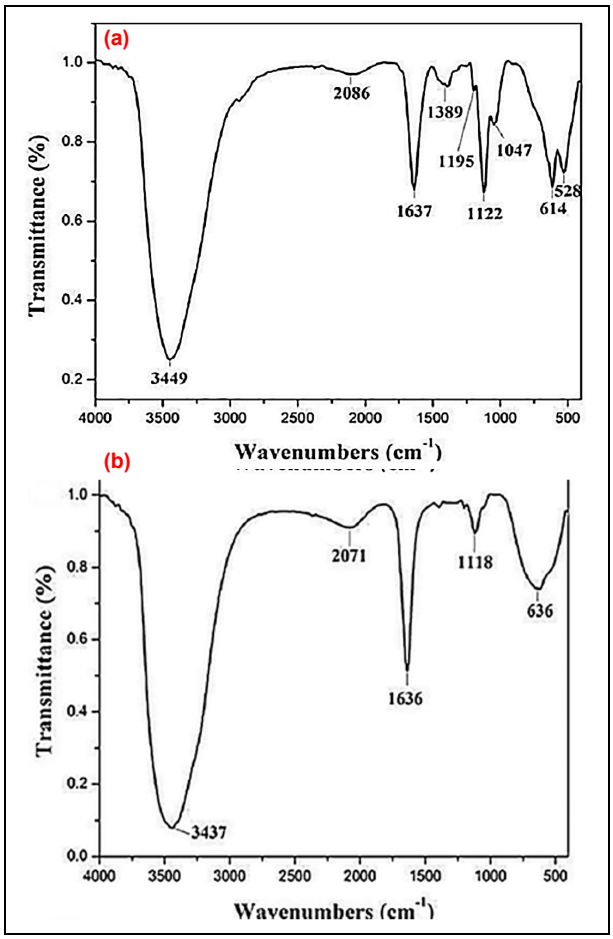


Fig. 5: (a) FT-IR spectrum of PN leaves extract (b) FT-IR spectrum of PN-CNDs

Table 2 demonstrates that as the concentration of PN-CNDs increases, the corrosion potential (E_{corr}) exhibits a modest positive shift while the corrosion current density (i_{corr}) decreases noticeably. The slight positive shift of E_{corr} suggests that the geometric blocking effect is mostly responsible for the inhibitory impact of PN-CNDs. Furthermore, the addition of PN-CNDs in a 1.0 M HCl solution appears to suppress both the anodic

dissolution and cathodic reduction reactions, with the anodic reaction being inhibited more successfully. In the meantime, when the concentration of PN-CNDS rises, so does the inhibition efficiency. According to the results above, PN-CNDs can function as a mixed-type inhibitor. Nearly parallel polarization curves for the cathodic portion of polarization curves show that the proton reduction mechanism is still in charge of the cathodic process. Nevertheless, the cathodic reduction reaction can be successfully inhibited by blocking the active sites using PN-CNDs that are adsorbed onto the surface of mild steel. When the potential is less than -0.33 V (*vs.* Ag/AgCl), the i_{corr} clearly declines in the case of the anodic branch of polarization curves, indicating the production of a protective PN-CNDs coating on the steel surface. The desorption of PN-CNDs from the steel surface causes the anodic current density in the presence of PN-CNDs to correspond with that in a blank solution after the polarization potential exceeds −0.33 V (*vs.* Ag/AgCl).

Table 2. Electrochemical characteristics derived from mild steel polarization curves in 1.0 M HCl with and without varying PN-CNDs concentrations

C (ppm)	E_{corr} (mV)	i_{corr} (µA cm^{-2})	β_c ($mVdec^{-1}$)	β_a ($mVdec^{-1}$)	η (%)
Blank	-445	647	-149.6	125.6	-
50	-442	182	-110.1	68.3	71.7
100	-439	89.5	-101.3	53.7	86.1
200	-433	54.7	-101.1	51.1	91.5
400	-430	23.2	-101.8	48.7	96.4

3.3.2 Impedance Studies

The corrosion behavior of mild steel in 1.0 M HCl solution with and without varying amounts of PN-CNDs was assessed using the EIS test after three hours of immersion at room temperature. As can be seen in Fig. 6b, Nyquist plots of all specimens, with or without PN-CNDs show a depressed capacitive arc at high and medium frequencies that corresponds to the charge transfer process (Simsek *et al*. 2019). The specimen's roughness and inhomogeneity are the reasons for the depressed capacitive arc shape. It is important to note that all EIS plots show comparable shapes whether PN-CNDs are present or not. This suggests that adding PN-CNDs to an HCl solution only prevents the charge transfer process by forming a protective layer by adsorbing onto the steel surface. It does not alter the electrochemical reaction mechanism. The lone pair of electrons present in the phyto-chemical constituents bind with weak force of attractions on the metal surface. Chemically it is known as the physisorption process.

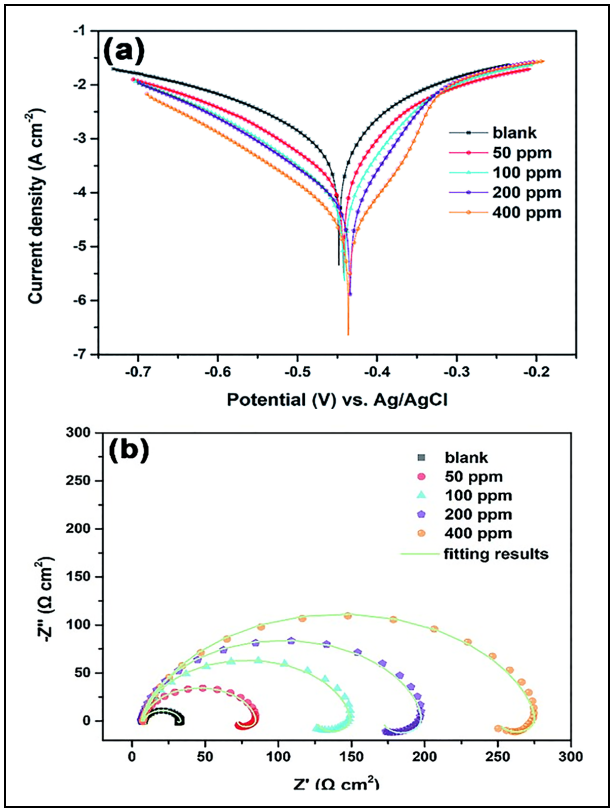


Fig. 6: (a) Potentiodynamic polarization curves (b) EIS measurement curves

Table 3. Electrochemical parameters derived from mild steel EIS data in a 1.0 M HCl solution with and without varying PN-CNDs concentrations

C (ppm)	R_{ct}, (Ω cm^2)	CPE_{dl}, (µF cm^{-2})	η (%)
Blank	23.76	263.00	-
50	76.32	110.02	58.16
100	146.94	72.80	72.31
200	194.42	52.93	79.87
400	276.40	33.58	87.23

The analogous circuit depicted in Fig. 6b is suggested to suit the EIS results in accordance with the previously given EIS results. The solution resistance in the equivalent circuit is denoted by R_s, while the charge-transfer resistance and double layer capacitance are represented by R_{ct} and CPE_{dl}, respectively. Because of the surface's inhomogeneity, CPE is used instead of the ideal capacitor. According to earlier reports, Brug's formula in the equation is used to determine the double layer capacitance (C_{dl}) value.

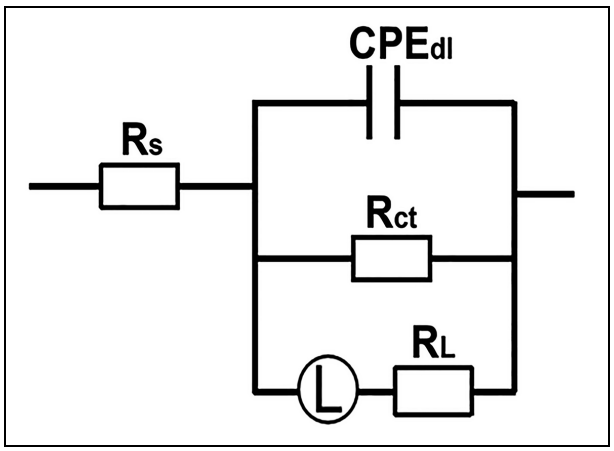


Fig. 7: Equivalent circuit used to fit the EIS results in Fig. 6b

$$C_{dl} = Y_0^{\frac{1}{n}} \left(\frac{1}{R_s} + \frac{1}{R_{ct}}\right)^{(n-1)/n} \quad \ldots (2)$$

where Y_0 is the magnitude of CPE and n corresponds to a phase shift ($-1 \leq n \leq 1$).

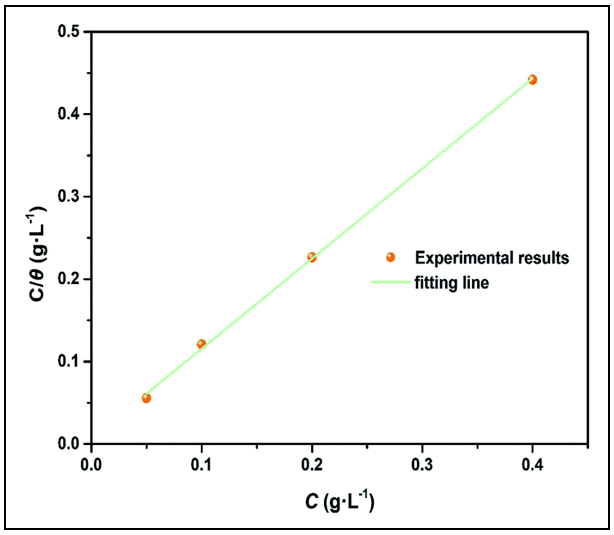


Fig. 8: Plot of Langmuir adsorption isotherm

Table 3 summarizes the fitting electrochemical parameters derived from the EIS data. As the concentration of PN-CNDs increases, the R_{ct} value rises from 23.76 Ω cm^2 to 276.40 Ω cm^2, whereas the C_{dl} value falls. The interaction of PN-CNDs with the steel surface's active sites rather than hydrogen bonding with water molecules is thought to be the cause of the drop in the C_{dl} value. Additionally, the following formulae (3-4) were used to determine the Electrical capacity of a binary layer and inhibitory efficiency:

$$C_{d.l} = 1/2\pi R_{ct} f_{max} \quad \ldots (3)$$

$$(\%\ I.E) = ((C_{d.l})_{acid} - (C_{d.l})_{PN\text{-}CNDs}/(C_{d.l})_{acid}) \times 100 \quad \ldots (4)$$

$(C_{d.l})_{acid}$ = Electrical capacity of a binary layer in acid

$(C_{d.l})_{PN\text{-}CNDs}$ = Electrical capacity of binary layer in acid + PN-CNDs,

where the charge transfer resistance in the presence and absence of PN-CNDs is denoted by R^0_{ct} and R_{ct}, respectively. Table 3 shows that the inhibition effectiveness increases dramatically as the concentration of PN-CNDs increases. The maximum inhibition efficiency, which is in good agreement with those in Table 2, is around 96.4% at 400 ppm PN-CNDs.

3.3.3 Adsorption Isotherm

The analysis indicates that the primary mechanism for preventing corrosion is the adsorption of PN-CNDs onto the steel surface. Therefore, understanding the interaction between PN-CNDs and mild steel is essential. In general, there are three categories of inhibitor adsorption. In this study, the Langmuir adsorption isotherm (Tabaraki and Sadeghinejad, 2018) results were obtained, which are represented by the following equation:

$$\frac{C_{inh}}{\theta} = C_{inh} + \frac{1}{K_{ads}} \quad \ldots (4),$$

where θ is the surface coverage, which may be computed using the above equation, K_{ads} is the adsorption equilibrium constant, and C_{inh} is the PN-CNDs concentration. The link between and C_{inh} is seen in Fig. 8. The plot intercept indicates that the K_{ads} value is 157.73 Lg^{-1}, which suggests that PN-CNDs have a significant adsorption on the steel surface. Furthermore, the adsorption of PN-CNDs appears to follow the Langmuir adsorption isotherm, as indicated by the regression coefficient (R^2) of 0.9999. The PN-CNDs contains the phytochemical components shown in Fig.4. The heteroatoms and aromatic rings in the organic compounds interact with the mild steel surface and form a protective layer which is confirmed by impedance studies. The Langmuir model clearly depicts the surface covered by the phytochemical components on the mild steel surface. Langmuir Adsorption Isotherm predicts linear adsorption at a maximum surface coverage and low adsorption densities. It happens at higher solute metal concentrations. It indicates the level of interaction between the surface and the adsorbate. If the value of this constant is larger, it indicates a strong interaction between the adsorbent and the adsorbate. On the other hand, K having a smaller value indicates a weaker interaction between the surface and the adsorbate. Langmuir clearly gives the foundation regarding adsorption of phyto-components in form of CNDs. Adsorption isotherms describe the relationship between the amount of adsorbate and its concentration in the solution at equilibrium, which is crucial for understanding the efficiency and nature of the adsorption process.

3.3.4 Morphology

Scanning electron microscopy was used to examine the steel surface's corrosion (Dhayabaran *et al*. 2004) condition following immersion in the tested solutions. Prior to immersion, the polished mild steel has a comparatively even and smooth surface, as seen in Fig. 9a. The surface of mild steel corrodes badly along the polished direction and becomes extremely coarse when it is exposed to the blank solution (Fig. 9b). Steel surface corrosion occurs in the polished direction when PN-CNDs are present, although the degree of corrosion is clearly reduced as the concentration of PN-CNDs rises (Fig. 9c).

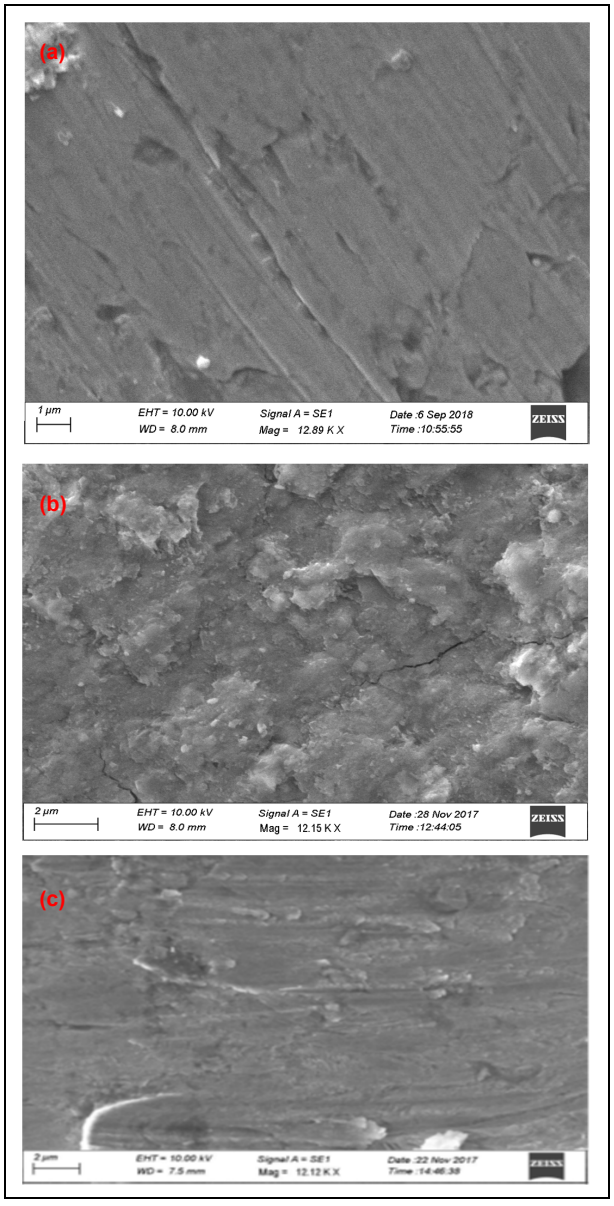


Fig. 9: (a) SEM micrograph for polished mild steel, (b) SEM micrograph for mild steel dipped in 1.0 M HCl, and (c) SEM micrograph for mild steel dipped in HCl/400 ppm of PN-CNDs

4. MECHANISM OF SURFACE FUNCTIONALIZATION BY PN-CNDS

A potential model to depict the inhibitory mechanism of PN-CNDs is put forth based on the previously indicated analysis of experimental data. It is commonly known that the adsorbed water molecules are always replaced to achieve the adsorption of inhibitor molecules onto the metal surface. The presence of nitrogen atoms in the blank solution causes PN-CNDs to become protonated in equilibrium. In addition, there is always a positive excess charge on the steel surface in the HCl solution. Through electrostatic interaction, which can serve as connecting bridge to promote the adsorption of protonated PN-CNDs on the positively charged steel surface, the hydrated chloride ions are selectively adsorbed onto the steel surface with positive charges. The reaction rate of hydrogen evolution would thus be lowered as a result of protonated PN-CNDs adsorbed onto the steel surface competing with hydrogen ions (Yuan *et al*. 2015; Yang *et al*. 2019). The FT-IR results show that the heteroatoms (N and O) in PN-CNDs exist in both single and multiple bond forms in addition to physisorption. This allows the PN-CNDs to readily adsorb onto the steel surface by forming coordinated bonds with Fe atoms and lone pair electrons. PN-CNDs might therefore successfully stop acid corrosion in mild steel.

5. CONCLUSION

The findings of the study demonstrate that PN-CNDs synthesized through a green hydrothermal approach using *Phyla nodiflora* leaves serve as a sustainable, renewable, and cost-effective source for carbon nanodot production. The developed PN-CNDs exhibited remarkable potential as environmentally friendly corrosion inhibitors for mild steel in 1.0 M HCl solution. Electrochemical studies confirmed their high inhibition efficiency, which increased with concentration and reached 96.4% at 400 ppm, outperforming many conventional inhibitors due to the abundance of active organic compounds present in the green CNDs. Characterization through UV-visible, FT-IR, and fluorescence analyses verified the successful synthesis of PN-CNDs. Adsorption studies revealed that the inhibition process occurred mainly through physisorption and followed the Langmuir adsorption isotherm. Furthermore, reduced corrosion damage and lower surface roughness of mild steel substantiated their excellent protective performance. The adsorption of PN-CNDs on the steel surface was attributed to the formation of a stable protective layer through the interaction of lone pair electrons from phytochemical constituents. Thus, PN-CNDs represent a promising, eco-friendly, and highly efficient alternative for corrosion protection applications.

ACKNOWLEDGMENT

The authors are grateful to the organization and the instrumentation conveniences sponsored by the DBT-Star College Scheme and Seed Money Project Scheme to complete their research work.

CONTRIBUTIONS

Mushira Banu Ahmed Meeran: Conceptualization, Funding acquisition, Investigation, Methodology, Project administration, Visualization, Writing, Original Draft; Arifa Farzana Bijili: Resources, Writing, Validation; Jayathivya: Conceptualization, Methodology; Kathiravan: Resources.

FUNDING

This research received no specific grant from any funding agency in the public, commercial, or nonprofit sectors.

CONFLICT OF INTEREST

The authors declared no conflict of interest in this manuscript regarding publication.

COPYRIGHT

This article is an open-access article distributed under the terms and conditions of the Creative Commons Attribution (CC BY) license (http://creativecommons.org/licenses/by/4.0/).

REFERENCES

Amjad, M., Iqbal, M., Faisal, A., Junjua, A. M., Hussain, I., Hussain, S. Z., Ghramh, H. A., Khan, K. A. and Janjua, H. A., Hydrothermal synthesis of carbon nanodots from bovine gelatin and PHM3 microalgae strain for anticancer and bioimaging applications, *Nanoscale Adv.*, 1(8), 2924–2936 (2019). https://doi.org/10.1039/C9NA00164F

Banu, A. M., Farzana, B. A., MujafarKani, N., Thakur, A., Ahamed, K. R. and Kumar, A., Microwave-assisted synthesis of carbon nanodots from Bombax ceiba leaves for enhanced Tribo-corrosion resistance: An experimental and computational analysis, *Results Surf. Interfaces*, 17100329 (2024). https://doi.org/10.1016/j.rsurfi.2024.100329

Bhunia, S. K., Saha, A., Maity, A. R., Ray, S. C. and Jana, N. R., Carbon Nanoparticle-based Fluorescent Bioimaging Probes, *Sci. Rep.*, 3(1), 1473 (2013). https://doi.org/10.1038/srep01473

Chan, K. K., Yap, S. H. K. and Yong, K. T., Biogreen Synthesis of Carbon Dots for Biotechnology and Nanomedicine Applications, *Nano-Micro Lett.*, 10(4), 72 (2018). https://doi.org/10.1007/s40820-018-0223-3

De, B. and Karak, N., Recent progress in carbon dot–metal based nanohybrids for photochemical and electrochemical applications, *J. Mater. Chem. A*, 5(5), 1826–1859 (2017). https://doi.org/10.1039/C6TA10220D

Dhayabaran, V. V., Merlin, J. P., Lydia, I. S., Shanthi, R. and Sivaraj, R., Inhibition of corrosion of aluminium in presence of fluorescein in basic medium, *Ionics*, 10(3–4), 288–290 (2004). https://doi.org/10.1007/BF02382831

Gao, D., Zhao, H., Chen, X. and Fan, H., Recent advance in red-emissive carbon dots and their photoluminescent mechanisms, *Mater. Today Chem.*, 9103–113 (2018). https://doi.org/10.1016/j.mtchem.2018.06.004

Genc, R., Alas, M. O., Harputlu, E., Repp, S., Kremer, N., Castellano, M., Colak, S. G., Ocakoglu, K. and Erdem, E., High-Capacitance Hybrid Supercapacitor Based on Multi-Colored Fluorescent Carbon-Dots, *Sci. Rep.*, 7(1), 11222 (2017). https://doi.org/10.1038/s41598-017-11347-1

Guo, X., Zhang, L., Wang, Z., Sun, Y., Liu, Q., Dong, W. and Hao, A., Fluorescent carbon dots based sensing system for detection of enrofloxacin in water solutions, *Spectrochim. Acta. A. Mol. Biomol. Spectrosc.*, 21915–22 (2019). https://doi.org/10.1016/j.saa.2019.02.017

He, G., Shu, M., Yang, Z., Ma, Y., Huang, D., Xu, S., Wang, Y., Hu, N., Zhang, Y. and Xu, L., Microwave formation and photoluminescence mechanisms of multi-states nitrogen doped carbon dots, *Appl. Surf. Sci.*, 422257–265 (2017). https://doi.org/10.1016/j.apsusc.2017.05.036

Jeong, C. J., Lee, G., In, I. and Park, S. Y., Concentration-mediated multicolor fluorescence polymer carbon dots, *Luminescence*, 31(3), 897–904 (2016). https://doi.org/10.1002/bio.3050

Jhonsi, M. A., Ananth, D. A., Nambirajan, G., Sivasudha, T., Yamini, R., Bera, S. and Kathiravan, A., Antimicrobial activity, cytotoxicity and DNA binding studies of carbon dots, *Spectrochim. Acta. A. Mol. Biomol. Spectrosc.*, 196295–302 (2018). https://doi.org/10.1016/j.saa.2018.02.030

Jiang, K., Sun, S., Zhang, L., Lu, Y., Wu, A., Cai, C. and Lin, H., Red, Green, and Blue Luminescence by Carbon Dots: Full-Color Emission Tuning and Multicolor Cellular Imaging, *Angew. Chem. Int. Ed.*, 54(18), 5360–5363 (2015). https://doi.org/10.1002/anie.201501193

Khan, Z. M. S. H., Rahman, R. S., Shumaila., Islam, S. and Zulfequar, M., Hydrothermal treatment of red lentils for the synthesis of fluorescent carbon quantum dots and its application for sensing Fe3+, *Opt. Mater.*, 91386–395 (2019). https://doi.org/10.1016/j.optmat.2019.03.054

Li, L., Wang, X., Fu, Z. and Cui, F., One-step hydrothermal synthesis of nitrogen- and sulfur-co-doped carbon dots from ginkgo leaves and application in biology, *Mater. Lett.*, 196300–303 (2017). https://doi.org/10.1016/j.matlet.2017.03.112

Liu, H., Ding, J., Zhang, K. and Ding, L., Construction of biomass carbon dots based fluorescence sensors and their applications in chemical and biological analysis, *TrAC Trends Anal. Chem.*, 118315–337 (2019). https://doi.org/10.1016/j.trac.2019.05.051

Meng, W., Bai, X., Wang, B., Liu, Z., Lu, S. and Yang, B., Biomass-Derived Carbon Dots and Their Applications, *ENERGY Environ. Mater.*, 2(3), 172–192 (2019). https://doi.org/10.1002/eem2.12038

Moradi, S., Sadrjavadi, K., Farhadian, N., Hosseinzadeh, L. and Shahlaei, M., Easy synthesis, characterization and cell cytotoxicity of green nano carbon dots using hydrothermal carbonization of Gum Tragacanth and chitosan bio-polymers for bioimaging, *J. Mol. Liq.*, 259284–290 (2018). https://doi.org/10.1016/j.molliq.2018.03.054

Naik, V. M., Gunjal, D. B., Gore, A. H., Pawar, S. P., Mahanwar, S. T., Anbhule, P. V. and Kolekar, G. B., Quick and low cost synthesis of sulphur doped carbon dots by simple acidic carbonization of sucrose for the detection of Fe3+ ions in highly acidic environment, *Diam. Relat. Mater.*, 88262–268 (2018). https://doi.org/10.1016/j.diamond.2018.07.018

Ogi, T., Aishima, K., Permatasari, F. A., Iskandar, F., Tanabe, E. and Okuyama, K., Kinetics of nitrogen-doped carbon dot formation via hydrothermal synthesis, *New J. Chem.*, 40(6), 5555–5561 (2016). https://doi.org/10.1039/C6NJ00009F

Quraishi, M. A., Singh, A., Singh, V. K., Yadav, D. K. and Singh, A. K., Green approach to corrosion inhibition of mild steel in hydrochloric acid and sulphuric acid solutions by the extract of Murraya koenigii leaves, *Mater. Chem. Phys.*, 122(1), 114–122 (2010). https://doi.org/10.1016/j.matchemphys.2010.02.066

Simsek, S., Ozge Alas, M., Ozbek, B. and Genc, R., Evaluation of the physical properties of fluorescent carbon nanodots synthesized using Nerium oleander extracts by microwave-assisted synthesis methods, *J. Mater. Res. Technol.*, 8(3), 2721–2731 (2019). https://doi.org/10.1016/j.jmrt.2019.04.008

Tabaraki, R. and Sadeghinejad, N., Microwave assisted synthesis of doped carbon dots and their application as green and simple turn off–on fluorescent sensor for mercury (II) and iodide in environmental samples, *Ecotoxicol. Environ. Saf.*, 153101–106 (2018). https://doi.org/10.1016/j.ecoenv.2018.01.059

Yang, P., Zhu, Z., Chen, M., Zhou, X. and Chen, W., Microwave-assisted synthesis of polyamine-functionalized carbon dots from xylan and their use for the detection of tannic acid, *Spectrochim. Acta. A. Mol. Biomol. Spectrosc.*, 213301–308 (2019). https://doi.org/10.1016/j.saa.2019.01.043

Yuan, M., Zhong, R., Gao, H., Li, W., Yun, X., Liu, J., Zhao, X., Zhao, G. and Zhang, F., One-step, green, and economic synthesis of water-soluble photoluminescent carbon dots by hydrothermal treatment of wheat straw, and their bio-applications in labeling, imaging, and sensing, *Appl. Surf. Sci.*, 3551136–1144 (2015). https://doi.org/10.1016/j.apsusc.2015.07.095

Zhang, J. and Yu, S. H., Carbon Dots: Large-Scale Synthesis, Sensing, and Bioimaging, *Mater. Today*, 19, 382–393 (2016). https://doi.org/10.1016/j.mattod.2015.11.008

Zhao, C., Li, X., Cheng, C. and Yang, Y., Green and Microwave-Assisted Synthesis of Carbon Dots and Application for Visual Detection of Cobalt (II) Ions and pH Sensing, *Microchem. J.*, 147, 183–190 (2019). https://doi.org/10.1016/j.microc.2019.03.029